Parameter Plane Analysis of Fuzzy Vehicle Steering Control Systems

JAU-WOEI PERNG, HUNG-I CHIN and BING-FEI WU
Department of Electrical and Control Engineering
National Chiao Tung University
1001, Ta Hsueh Road, Hsinchu,300
TAIWAN, R.O.C.

Abstract: - The main purpose of this paper is to analyze the robust stability for a fuzzy vehicle steering control system. In general, fuzzy control system is a nonlinear control system. Therefore, the fuzzy controller may be linearized by the use of describing function first. After then, parameter plane method is then applied to determine the conditions of robust stability when the system has perturbed or adjustable parameters. A systematic procedure is proposed to solve this problem. The effects of plant parameters and control factors are both considered here. Furthermore, the problem of relative stability by using gain-phase margin tester is also addressed. The limit cycles provided by a static fuzzy controller can be easily suppressed if the control factors are chosen properly. Simulation results show the efficiency of our approach.

Key-Words:- Vehicle steering system, fuzzy control, parameter plane, limit cycle, gain-phase margins, describing function.

1 Introduction

The describing function is a useful frequency domain approach for analyzing the stability of a nonlinear control system especially when the system has hard nonlinear elements, such as relay, deadzone, saturation, backlash, hysteresis and so on. The definition of describing function can be obtained from some reference books [1,2]. The applications of describing function have been widely developed in the academic and industry researches. For multivariable process control, a method for automatically tuning multivariable PID controllers from relay feedback was proposed in [3]. The describing function utilized for the stability analysis and limit cycle prediction of nonlinear control systems has been developed in [4]. The hysteresis describing function was applied to the class AD audio amplifier for modeling the inverter [5]. Recently, Chung et al [6] used the describing function method to linearise the nonlinear inductor and estimate the inductance in large current situations. Ackermann and Bunte [7] employed the describing function to predict the limit cycles in the parameter plane of velocity and road tire friction coefficient. In addition, some researchers have developed the experimental and analytic describing functions of fuzzy controller in order to analyze the stability of fuzzy control systems [8,9]. Furthermore, the describing function technique to design a fuzzy controller for switching DC-DC regulators was proposed by Gomariz et al [10]. The describing function was also applied to find the bounds for the neural network parameters to have a stable system response and generate limit cycles [11]. Generally speaking, the uncertainties are often existed in the practical control systems. It is well known that the frequency domain algorithms of parameter plane and parameter space [12-13] have been applied to fulfill the robust stability of an interval polynomial.

In this paper, we extend the results in [9,10] to analyze the stability of a fuzzy vehicle steering control system under the effects of system parameters and gain-phase margins by the use of methods of describing function, parameter plane and gain-phase margin tester. A simple vehicle steering control model with perturbed parameters is cited to verify the design procedure.

2 Problem Formulation

In this section, the classical linearized single track vehicle model is given first. The describing function of static fuzzy controller is also introduced. In order to analyze the stability of perturbed parameters, a systematic procedure is proposed to solve this problem by the use of parameter plane method and gain-phase margin tester.

2.1 Vehicle model [7]

Fig. 1 shows the single track vehicle model and the related symbols are listed in Table 1. The equations of motion are

$$\begin{bmatrix} mv(\dot{\beta}+r) \\ ml_f l_r \dot{r} \end{bmatrix} = \begin{bmatrix} F_f + F_r \\ F_f l_f - F_r l_r \end{bmatrix} \quad (1)$$

The tire force can be expressed as

$$F_f(\alpha_f) = \mu c_{f0}\alpha_f, \quad F_r(\alpha_r) = \mu c_{r0}\alpha_r \quad (2)$$

with the tire cornering stiffnesses c_{f0}, c_{r0}, the road adhesion factor μ and the tire side slip angles

$$\alpha_f = \delta_f - (\beta + \frac{l_f}{v}r), \alpha_r = -(\beta - \frac{l_r}{v}r) \quad (3)$$

The state equation of vehicle dynamics with β and r can be represented as

$$\begin{bmatrix} \dot{\beta} \\ \dot{r} \end{bmatrix} = \begin{bmatrix} -\frac{\mu(c_{f0}+c_{r0})}{mv} & -1+\frac{\mu(c_{r0}l_r - c_{f0}l_f)}{mv^2} \\ \frac{\mu(c_{r0}l_r - c_{f0}l_f)}{ml_f l_r} & -\mu\frac{(c_{f0}l_f^2 + c_{r0}l_r^2)}{ml_f l_r v} \end{bmatrix} \begin{bmatrix} \beta \\ r \end{bmatrix} + \begin{bmatrix} \frac{\mu c_{f0}}{mv} \\ \frac{\mu c_{f0}}{ml_r} \end{bmatrix} \delta_f \quad (4)$$

Hence, the transfer function from δ_f to r is

$$G_{r/\delta_f} = \frac{c_{f0}ml_f\mu v^2 s + c_{f0}c_{r0}l\mu^2 v}{l_f l_r m^2 v^2 s^2 + l(c_{r0}l_r + c_{f0}l_f)m\mu v s + c_{f0}c_{r0}l^2\mu^2 + (c_{r0}l_r - c_{f0}l_f)m\mu v^2} \quad (5)$$

The numerical data in this paper are listed in Table 2. According to the above analysis of a single track vehicle model, the transfer function from the input of front deflection angle δ_f to the output of yaw rate r can be obtained as

$$G_{r/\delta_f}(s,\mu,v) = \frac{(1.382\times10^8\mu v^2 s + 1.415\times10^{10}\mu^2 v)}{6.675\times10^6 v^2 s^2 + 1.08\times10^9\mu v s + (1.034\times10^7\mu v^2 + 4\times10^{10}\mu^2)} \quad (6)$$

The operating range Q of the uncertain parameters μ and v is depicted in Fig. 2.

In addition, the steering actuator is modeled as

$$G_A(s) = \frac{\omega_n^2}{s^2 + \sqrt{2}\omega_n s + \omega_n^2} \quad (7)$$

where $\omega_n = 4\pi$.

In our study, a fuzzy vehicle control system is presented in Fig. 3. The open loop transfer function $G_O(s)$ is defined as

$$G_O(s,\mu,v) = G_A(s)G_{r/\delta_f}(s,\mu,v) \quad 8)$$

The control factors k_p, k_d and k_u can be determined by the designer. By transferring Fig. 3 to Fig. 4, the overall open loop transfer function can be obtained as

$$G(s,k_p,k_d,k_u,\mu,v) = \frac{k_p + s\cdot k_d}{\sqrt{2}}\cdot\frac{k_u}{s}\cdot G_O(s,\mu,v) \quad (9)$$

2.2 Describing function of static fuzzy controller [9]

The describing function N_1 of static fuzzy controller shown in Fig. 4 can be obtained, which depends only on the amplitude of A and is independent of the frequency of ω, and can be expressed as follows:

$$\begin{aligned} N_1 &\triangleq N_1(A) \\ &= \frac{4}{\pi A}\sum_{i=0}^{n}\{\frac{\Delta u_i A}{2\Delta\Phi_i}((\delta_{i+1} - \sin\delta_{i+1}\cos\delta_{i+1}) \\ &\quad -(\delta_i - \sin\delta_i\cos\delta_i)) + \frac{1}{\Delta\Phi_i} \\ &\quad \cdot(\Phi_i u_{i+1} - \Phi_{i+1}u_i)(\cos\delta_{i+1} - \cos\delta_i)\}, \end{aligned} \quad (10)$$

where n satisfies $\Phi_n \le A < \Phi_{n+1}$, $n > 0$, and varies with A; new variables $\{\delta_i\}$ are defined to be the angles where the input sinusoidal signal $x = A\sin\delta$ intersects the centers of fuzzy membership functions (Φ_i's) as follows:

$$\delta_0 = 0,$$

$$\delta_i = \sin^{-1}\left(\frac{\Phi_i}{A}\right), \qquad \left(i = 1,\cdots,n, 0 < \delta_i < \frac{\pi}{2}\right),$$

$$\delta_{n+1} = \frac{\pi}{2}.$$

The detail definitions of n and δ_i's are visualized in [9].

2.3 Stability analysis of fuzzy vehicle control systems

If the gain-phase margin tester $Ke^{-j\theta}$ is added in the open loop of Fig. 4, the closed loop transfer function is

$$\frac{Ke^{-j\theta}N_1 G(s,k_p,k_d,k_u,\mu,v)}{1 + Ke^{-j\theta}N_1 G(s,k_p,k_d,k_u,\mu,v)} = 0 \quad (11)$$

Case 1: *Perturbed plant parameters*

Arrange (11), the following characteristic equation is obtained.

$$\begin{aligned} &f(s,k_p,k_d,k_u,\mu,v,K,\theta) \\ &= C_4\mu^2 + C_3 v^2 + C_2\mu v + C_1\mu^2 v + C_0\mu v^2 \\ &= 0 \end{aligned} \quad (12)$$

where

$$C_4 = 5.656\times10^{10}s(s^2 + 17.7668s + 157.9137),$$

$$C_3 = 9.4384\times10^6 s^3(s^2 + 17.7668s + 157.9137),$$

$$C_2 = 1.5271\times10^9 s^2(s^2 + 17.7668s + 157.9137),$$

$$C_1 = 2.2345\times10^{12}Ke^{-j\theta}N_1 k_u(k_p + k_d s),$$

$$C_0 = 1.4621\times10^8 s(s^2 + 17.7688s + 157.9137) + 2.1818\times10^{10}Ke^{-j\theta}N_1 k_u s(k_p + k_d s).$$

Let $s = j\omega$, $K = 0\,\text{dB}$ and $\theta = 0^\circ$. (12) is divided

into two stability equations with real part X_R and imaginary part X_I of characteristic equation, one has

$$f(j\omega, k_p, k_d, k_u, \mu, v) = X_R + jX_I = 0 \quad (13)$$

where

$$\begin{aligned} X_R = & -1.0064\times10^{12}\omega^2\mu^2 + 1.6776\times10^8\omega^4v^2 + \\ & (1.5179\times10^9\omega^4 - 2.3999\times10^{11}\omega^2)\mu v + \\ & 2.2345\times10^{12}N_1k_pk_u\mu^2v - (2.5986\times10^9\omega^2 + \\ & 2.1818\times10^{10}N_1k_dk_u\omega^2)\mu v^2, \\ X_I = & (8.9429\times10^{12}\omega - 5.656\times10^{10}\omega^3)\mu^2 + \\ & (9.4399\times10^6\omega^5 - 1.4907\times10^9\omega^3)v^2 - \\ & 2.7008\times10^{10}\omega^3\mu v + 2.2345\times10^{12}N_1k_dk_u\omega\mu^2v + \\ & (2.3091\times10^{10}\omega - 1.4621\times10^8\omega^3 + \\ & 2.1818\times10^{10}N_1k_pk_u\omega)\mu v^2. \end{aligned}$$

In order to obtain the solution of μ and v, the following equation is solved

$$\begin{cases} X_R = 0 \\ X_I = 0 \end{cases}, \quad (14)$$

when k_p, k_d, k_u, N_1 are fixed and ω is changed from 0 to ∞. As the amplitude A is also changed, the solutions of μ and v called limit cycle loci can be displayed in the parameter plane.

Case 2: Control factors

After some simple manipulations, the characteristic equation of (11) can be obtained as

$$f(s, k_p, k_d, k_u, \mu, v, K, \theta) = U\cdot k_p + V\cdot k_d + W = 0 \quad (15)$$

where

$$\begin{aligned} U &= Ke^{-j\theta}N_1k_u(2.1818\times10^{10}\mu v^2s + 2.2345\times10^{12}\mu^2v), \\ V &= Ke^{-j\theta}N_1k_us(2.1818\times10^{10}\mu v^2s + 2.2345\times10^{12}\mu^2v), \\ W &= 1.414s(s^2 + 17.7688s + 157.9137)(6.675\times10^6v^2s^2 + \\ & \quad 1.0746\times10^9\mu vs + 4.0045\times10^{10}\mu^2 + 1.034\times10^8\mu v^2). \end{aligned}$$

Let $s = j\omega$, $K = 0\,\text{dB}$ and $\theta = 0^\circ$. (15) is divided into two stability equations with real part and imaginary part of characteristic equation

$$f(j\omega, k_p, k_d, k_u, \mu, v) = X_R + jX_I = 0, \quad (16)$$

where

$$X_R = U_1\cdot k_p + V_1\cdot k_d + W_1 = 0, \quad (17)$$

and

$$X_I = U_2\cdot k_p + V_2\cdot k_d + W_2 = 0. \quad (18)$$

Therefore, k_p and k_d are solved from (14) and (15) when μ, v, k_u, N_1 are fixed and ω is changed from 0 to ∞, one has

$$k_p = \frac{V_1\cdot W_2 - V_2\cdot W_1}{U_1\cdot V_2 - U_2\cdot V_1}, \quad (16)$$

and

$$k_d = \frac{W_1\cdot U_2 - W_2\cdot U_1}{U_1\cdot V_2 - U_2\cdot V_1}. \quad (17)$$

Case 3:Gain-phase margin analysis

The gain-phase margin tester can be expressed as

$$Ke^{-j\theta} = K\cos\theta - jK\sin\theta = K_R - jK_I \quad (18)$$

where

$$K_R = K\cos\theta,$$

and

$$K_I = K\sin\theta.$$

It is noted that $K = \sqrt{K_R^2 + K_I^2}$ and $\theta = \tan^{-1}(\frac{K_I}{K_R})$.

Then, the characteristic equation can be written as

$$f(s, k_p, k_d, k_u, \mu, v, K_R, K_I) = U\cdot K_R + V\cdot K_I + W = 0 \quad (19)$$

where

$$\begin{aligned} U &= N_1k_u(2.1818\times10^{10}\mu v^2s + 2.2345\times10^{12}\mu^2v)(k_p + k_ds) \\ V &= (-j)N_1k_u(2.1818\times10^{10}\mu v^2s + 2.2345\times10^{12}\mu^2v)\times \\ & \quad (k_p + k_ds) \\ W &= 1.414s(s^2 + 17.7688s + 157.9137)(6.675\times10^6v^2s^2 + \\ & \quad 1.0746\times10^9\mu vs + 4.0045\times10^{10}\mu^2 + 1.034\times10^8\mu v^2). \end{aligned}$$

Let $s = j\omega$, (19) is divided into two stability equations with real part and imaginary part of characteristic equation

$$f(j\omega, k_p, k_d, k_u, \mu, v, K_R, K_I) = X_R + jX_I = 0, \quad (20)$$

where

$$X_R = U_1\cdot K_R + V_1\cdot K_I + W_1 = 0, \quad (21)$$

and

$$X_I = U_2\cdot K_R + V_2\cdot K_I + W_2 = 0. \quad (22)$$

Therefore, K_R and K_I are solved from (14) and (15) when k_p, k_d, μ, v, k_u, N_1 are fixed and ω is changed from 0 to ∞, one has

$$K_R = \frac{V_1\cdot W_2 - V_2\cdot W_1}{U_1\cdot V_2 - U_2\cdot V_1}, \quad (23)$$

and

$$K_I = \frac{W_1\cdot U_2 - W_2\cdot U_1}{U_1\cdot V_2 - U_2\cdot V_1}, \quad (24)$$

3 Simulation Rzesults

In our work, five fuzzy rules and parameters are adopted and listed in Tables 3 and 4, respectively. Fig. 5 shows the premise triangle membership functions of fuzzy controller. The consequent parts are singletons. Fig. 6 shows the control surface of fuzzy controller.

3.1 Plant parameter analysis

If $k_p = 0.2$, $k_d = 0.3$ and $k_u = 0.2$ are selected

first, (14) can be solved when A is fixed and ω is changed from 0 to ∞. Fig. 7 shows the stability boundary and some limit cycle loci in the μ-v parameter plane. Two stability regions including asymptotically stable and limit cycle are divided. In order to verify the accuracy of Fig. 7, four operating points Q1-Q3 (limit cycle region) and Q4 (asymptotically stable region) are illustrated for testing. Fig. 8 shows the time responses of input signal $x(t)$. It is obvious that the results shown in Fig. 8 consist with the predicted results in Fig. 7. For examples, if Q1($\mu = 1$ and $v = 70$) is chosen, the limit cycle occurs and the amplitude is 0.0465. Besides, if Q4 ($\mu = 1$ and $v = 5$) is chosen, the system is stable and no limit cycle happens. On the other hand, if $k_p = 0.1$, $k_d = 0.27$ and $k_u = 0.1$ are selected, Fig. 9 shows the stability boundary. We can find that no limit cycle will occur in the overall operating region Q (limit cycle free [7]).

If $k_u = 0.2$, $\mu = 1$ and $v = 70$ are selected, (19) and (20) can be solved in the k_p-k_d parameter plane when A is fixed and ω is changed from 0 to ∞. Fig. 10 shows the stability boundary and some limit cycle loci. Four testing points Q5-Q8 are illustrated.

If Q8 ($k_p = 0.1$, $k_d = 0.1$, $k_u = 0.2$, $\mu = 1$, $v = 70$) in Fig. 10 is selected, (23) and (24) can be solved in the K_R-K_I parameter plane when A is fixed and ω is changed from 0 to ∞. Because Q8 is in asymptotically stable region, the gain-phase margin tester can be viewed as a compensator to generate the limit cycle (from stable region to limit cycle region). For example, if $A = 0.05$ is expected, the related gain margin (Q9: $\mathrm{GM} = 3.2$, $\theta = 0^\circ$) and phase margin (Q10: $\mathrm{PM} = 46.6^\circ$, $K = 1$) to generate limit cycles can be easily obtained in Fig. 11. On the other hand, when the original system is in limit cycle region like Q5-Q7, the related gain margin and phase margin to suppress limit cycle could be also obtained in the parameter plane.

4 Conclusion

Based on the parameter plane approach, the complete stability analysis of a fuzzy vehicle steering control system is proposed in this paper. A systematic procedure is presented to deal with this problem. In addition, the effects of control factor and gain-phase margins are also considered. Simulation results show that more information can be obtained by this approach.

Reference:

[1] D. D. Siljak, *Nonlinear Systems - The Parameter Analysis and Design*, New York: Wiley, 1969.

[2] K. W. Han, *Nonlinear Control Systems - Some Practical Methods*, Academic Cultural Company, California, 1977.

[3] Q. G. Wang, B. Zou and T. H. Lee and Q. Bi, "Auto-tuning of Multivariable PID Controllers from Decentralied Relay Feedback," *Automatica*, Vol 33. No. 3, 1997, pp. 319-330.

[4] R. K. Miller, A. N. Michel and G. S. Krenz, "On the Stability of Limit Cycles in Nonlinear Feedback Systems: Analysis Using Describing Functions," *IEEE Trans. Circuits and Systems*, Vol. CAS-30, No. 9, 1983, pp.684-696.

[5] A. E. Ginart, R. M. Bass, W. M. Leach. Jr, and T. G. Habetler, "Analysis of the Class AD Audio Amplifier Including Hysteresis Effects," *IEEE Trans. Power Electronics*, Vol. 18, No. 2, 2003, pp.679-685.

[6] S. C. Chung, S. R. Huang, J. S. Huang and E. C. Lee, "Applications of Describing Functions to Estimate the Performance of Nonlinear Inductance," *IEE Proc. Sci. Meas. Techno*l., Vol. 148, No. 3, 2001, pp. 108-114.

[7] J. Ackermann and T. Bunte, "Actuator Rate Limits in Robust Car Steering Control," *Proc. IEEE Conf. Decision. and Control*, 1997, pp. 4726-4731.

[8] F. Gordillo, J. Aracil and T. Alamo, "Determining Limit Cycles in Fuzzy Control Systems," *Proc. IEEE Int. Conf. Fuzzy Syst.*, Vol. 1, 1997, pp. 193-198.

[9] E. Kim, H. Lee and M. Park, "Limit-Cycle Prediction of a Fuzzy Control System Based on Describing Function Method," *IEEE Trans. Fuzzy Syst*., Vol. 8, No. 1, 2000, pp. 11-21.

[10] S. Gomariz, F. Guinjoan, E. V. Idiarte, L. M. Salamero and A. Poveda, "On the Use of the Describing Function in Fuzzy Controllers Design for Switching DC-DC Regulators," *IEEE Int. Symp. Circuits Syst*., Vol. 3, pp. 247-250.

[11] A. Delgado, "Stability Analysis of Neurocontrol Systems Using a Describing Function," *Proc. Int. Join. Conf. Neural Network*, Vol. 3, 1998, pp. 2126-2130.

[12] D. D. Siljak, "Parameter Space Methods for Robust Control Design: A Guide Tour," *IEEE Trans. Automat. Contr.*, Vol. 34, No. 7, 1989, pp. 674-688.

[13] K. W. Han and G. J. Thaler, "Control System Analysis and Design Using a Parameter Space Method," *IEEE Trans. Automat. Contr*., Vol. 11, No. 3, 1966, pp. 560-563.

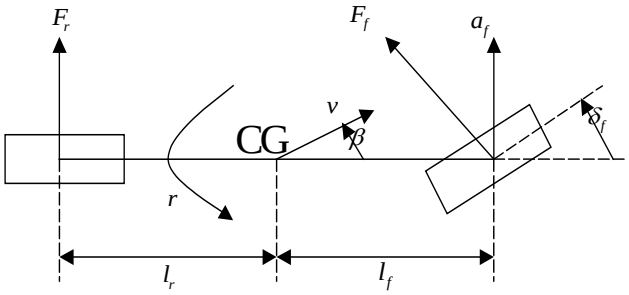

Fig. 1 Single track vehicle model.

TABLE I
VEHICLE SYSTEM QUANTITIES

F_f , F_r	lateral wheel force at front and rear wheel
r	yaw rate
β	side slip angle at center of gravity (CG)
v	velocity
a_f	lateral acceleration
l_f , l_r	distance from front and rear axis to CG
$l = l_f + l_r$	wheelbase
δ_f	front wheel steering angle
m	mass

TABLE II
VEHICLE SYSTEM PARAMETERS

c_{f0}	5000 N/rad
c_{r0}	100000 N/rad
m	1830 kg
l_f	1.51 m
l_r	1.32 m

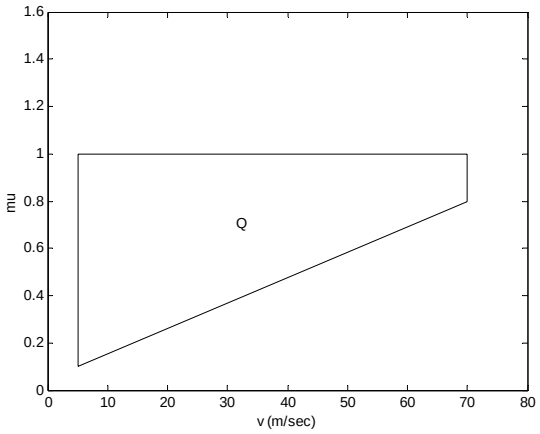

Fig. 2 Operating range.

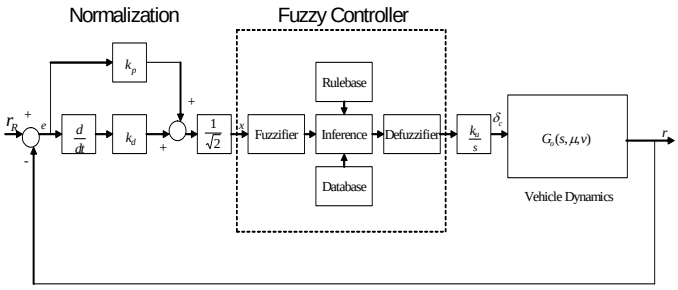

Fig. 3 Block diagram of fuzzy vehicle control system.

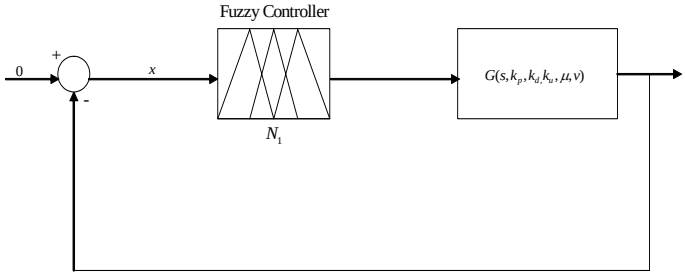

Fig. 4 Block diagram of fuzzy vehicle control system.

TABLE III
RULES OF FUZZY CONTROLLER

e	NBE	NSE	ZRE	PSE	PBE
u	NBU	NSU	ZRU	PSU	PBU

TABLE IV
PARAMETERS OF FUZZY CONTROLLER

e	nbe	nse	zre	pse	pbe
	-1	-0.02	0	0.02	1
u	nbu	nsu	zru	psu	pbu
	-1	-0.7	0	0.7	1

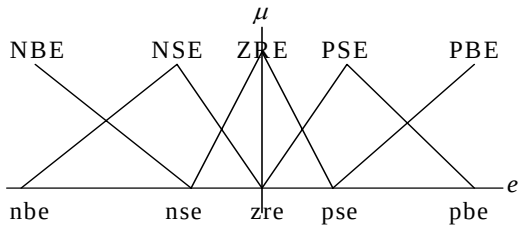

Fig. 5 Membership functions of fuzzy controller.

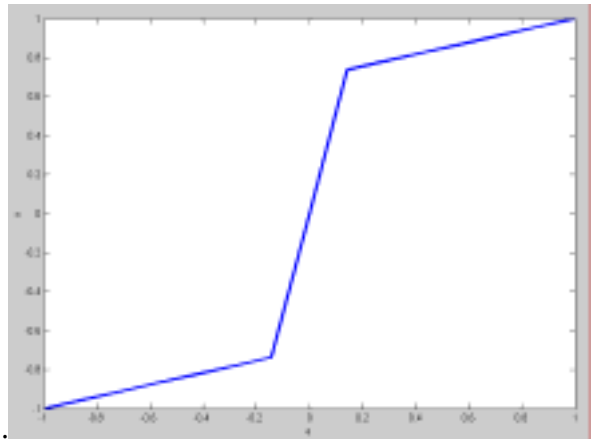

Fig. 6 Control surface.

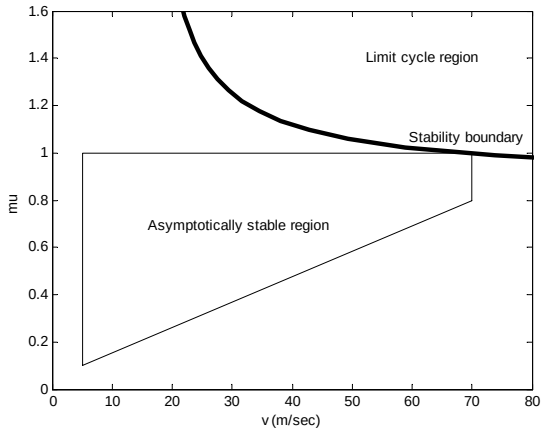

Fig. 9 Stability boundary.

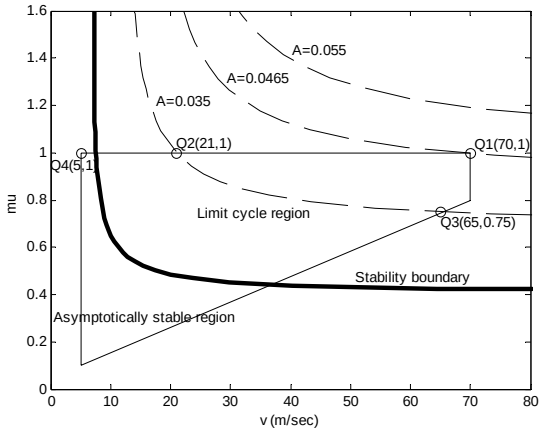

Fig. 7 Limit cycle loci.

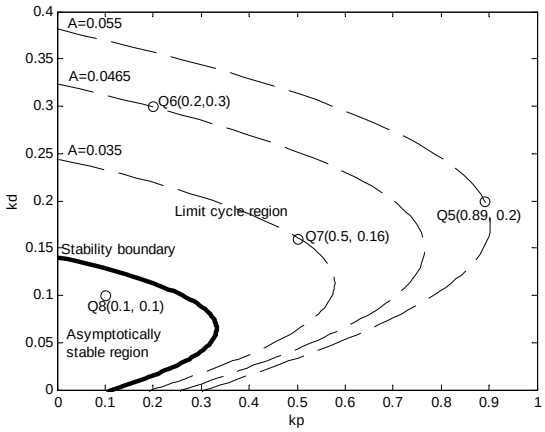

Fig. 10 Stability boundary.

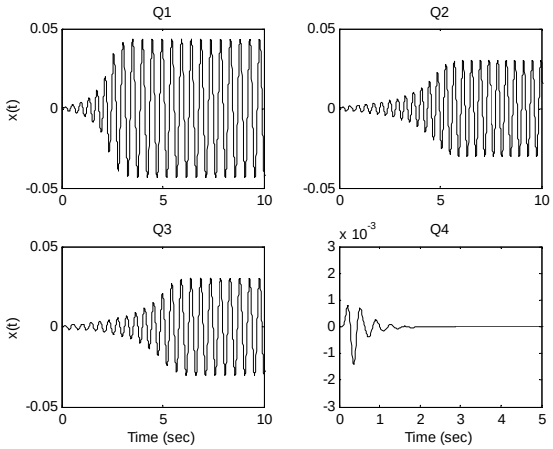

Fig. 8 Time responses of input signal.

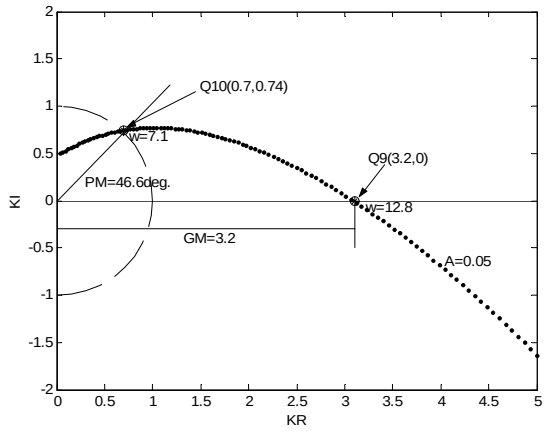

Fig. 11 GM and PM analysis.